



New host copolymers containing pendant triphenylamine and carbazole for efficient green phosphorescent OLEDs

Chih-Cheng Lee, Kun-Ming Yeh, Yun Chen*

Department of Chemical Engineering, National Cheng Kung University, Tainan, Taiwan

ARTICLE INFO

Article history:

Received 22 March 2008
Received in revised form 23 June 2008
Accepted 16 July 2008
Available online 23 July 2008

Keywords:

Polymerization
Light-emitting diodes (LEDs)
Luminescence

ABSTRACT

A series of vinyl copolymers (**P1–P6**) containing pendant hole-transporting triphenylamine (11–88 mol%) and carbazole chromophores were synthesized by radical copolymerization to investigate the influence of triphenylamine groups upon optoelectronic properties. The copolymers were readily soluble in common organic solvents and their weight-average molecular weights ($M_{w,s}$) were between 1.41×10^4 and 2.24×10^4 . They exhibited moderate thermal stability with $T_d = 402\text{--}432$ °C at 5% weight loss. The emission spectra (both PL and EL) of the blends [**P1–P6** with 4 wt% Ir(ppy)₃] showed dominant green emission (517 nm) attributed to Ir(ppy)₃ due to efficient energy transfer from **P1–P6** to Ir(ppy)₃. The HOMO levels of **P1–P6**, estimated from onset oxidation potentials in cyclic voltammeter, were -5.42 to -5.18 eV, which are much higher than -5.8 eV of conventional poly(9-vinylcarbazole) (**PVK**) host owing to high hole-affinity of the triphenylamine groups. The optoelectronic performances of phosphorescent EL devices, using **P1–P6** as hosts and Ir(ppy)₃ as dopant (ITO/PEDOT:PSS/**P1–P6**:Ir(ppy)₃ (4 wt%):PBD (40 wt%)/BCP/Ca/Al), were greatly improved relative to that of **PVK**. The best performance was obtained with **P4** device, in which the maximum luminance and luminance efficiency were 11501 cd/m² and 10.6 cd/A, respectively.

© 2008 Elsevier Ltd. All rights reserved.

1. Introduction

Since the report on electroluminescence of poly(*p*-phenylenevinylene) (PPV) by the Cambridge group [1], electroluminescent conjugated polymers have been intensively investigated and considered as one of the most promising materials for flat panel displays due to several advantages such as tunable color by molecular design, good processability by solution coating or ink-jetting, and good thermal stability. One of the limitations of the conventional fluorescence-based organic light-emitting diodes (OLEDs) and polymer light-emitting diodes (PLEDs) is that the radiation path for electron-hole recombination is limited to singlet excitons formed. However, organic phosphorescent LEDs based on heavy metal complexes from small organic molecules [2–6] and polymers [7–13] have attracted great attention currently due to the harvest of the both singlet and triplet excitons, which potentially can reach 100% internal quantum efficiency. Recently, the literatures of electroluminescent devices consisting of iridium [3], platinum [14], or ruthenium [15] metal complexes have been reported. The presence of heavy metal complexes would enhance phosphorescence because of the strong spin-orbit coupling that leads to

rapid intersystem crossing (ISC) and short triplet state lifetime [16]. Baldo et al. reported high efficiency phosphorescent LEDs by doping phosphorescent complex tris(2-phenylpyridine) iridium [Ir(ppy)₃] with small-molecular host material 4,4'-*N,N'*-dicarbazole-biphenyl [5]. Phosphorescent LEDs fabricated using a carbazole-based polymer, poly(9-vinylcarbazole) (**PVK**), as the general host material for the phosphorescent Ir(ppy)₃ dopant by simple solution process were reported [8–10]. Mechanistically, the photo-excited energy from the host material (**PVK**) transfers to phosphorescent dopant [Ir(ppy)₃] via Förster and/or Dexter transfer processes. For efficient Förster energy transfer to phosphorescent dopant, the spectral overlap between the photoluminescence (PL) band of the host material and the absorption band of the phosphorescent dopant is indispensable. For Dexter transfer process, relative position of triplet energy levels of the host materials and phosphor should be taken into account. If the triplet energy level of the phosphor is higher than that of the host, quenching of the excited triplet state in phosphor will occur through back energy transfer from triplet state in phosphor to that in host [17]. Of particular importance regarding the efficiency of phosphorescent LEDs is the selection of a proper host with high triplet state energy to guarantee the confinement of the excited states on the phosphorescent dyes [18]. Although several kinds of phosphorescent polymers possessing both host units and heavy metal complexes have been synthesized and discussed [19–22], complicated

* Corresponding author. Tel./fax: +886 6 2085843.
E-mail address: yunchen@mail.ncku.edu.tw (Y. Chen).

synthetic procedures and high cost impede their commercial development. Blending is one of the adaptable methods to circumvent this difficulty, although there still remain some intrinsic problems such as aggregation of the phosphor and inefficient energy transfer [23–25]. In addition, compared with phosphorescent polymers, accurate composition control of the hosts and phosphors is much easier for blend system.

Triphenylamine and its derivatives, such as 4,4'-bis(phenyl-*m*-tolylamino)biphenyl (TPD) and 4,4',4''-tris(*N,N*-diphenylamino)-triphenylamine (TDATA) [26,27], are effective electron donors and widely used as a hole-transporting materials in OLEDs and other optoelectronic applications. Recently, small-molecular host based on triphenylamine chromophore has been developed, i.e. 4,4',4''-tris(*N*-carbazolyl)triphenylamine (TCTA), which is a star-shaped molecule that consists of a triphenylamine core and three carbazolyl chromophores [28,29]. In order to enhance the hole transporting ability of the conventional PVK, we introduced the triphenylamine chromophore into the side chain by copolymerizing 9-vinylcarbazole and 4-vinyltriphenylamine. However, to the best of our knowledge, using copolymers based on triphenylamine and carbazole chromophores as the host material for the phosphorescent Ir(ppy)₃ dopant has not been attempted so far. In this work, we prepared a series of new vinyl copolymers (P1–P6) containing pendant triphenylamine and carbazole chromophores with a goal to develop effective host material for Ir(ppy)₃ dopant. Optical and electrochemical characteristics of P1–P6 were studied to confirm their potential suitability as host material. The blend films of hole-transporting host copolymers (P1–P6) and green phosphor [Ir(ppy)₃] were prepared by casting from their chlorobenzene solution. Composition-dependent photoluminescent (PL) and electroluminescent (EL) spectral properties of the blends were investigated in detail.

2. Experimental

2.1. Materials and measurements

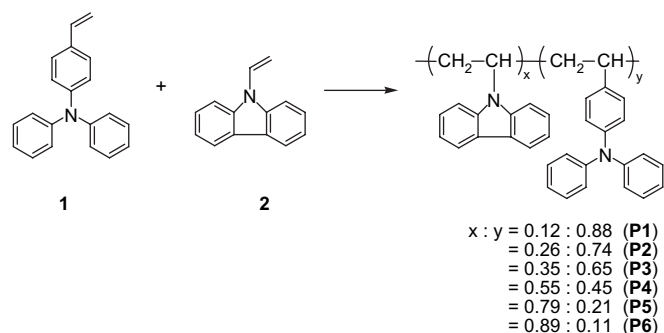
PVK and 2-(4-biphenyl)-5-(4-*tert*-butylphenyl)-1,3,4-oxadiazole (PBD) were purchased from Aldrich and used without further purification. Poly(4-vinyltriphenylamine) (PTPA) was prepared by free radical polymerization of 4-vinyltriphenylamine (**1**) [30]. 9-Vinylcarbazole (**2**) was purchased from Aldrich and purified by recrystallizing from ethanol/acetone and dried *in vacuo*. Iridium complexes Ir(ppy)₃ were purchased from American Dye Source (ADS). The vinyl copolymers P1–P6 were prepared by free radical copolymerization of 9-vinylcarbazole and 4-vinyltriphenylamine using AIBN as an initiator. AIBN was purified by recrystallizing twice from ethanol and dried at room temperature under vacuum. Other reagents were of commercial sources and used without further purification. The solvents were dried by the conventional procedures. All new compounds were identified by ¹H NMR, FT-IR, and elemental analysis (EA). The ¹H NMR spectra were recorded with a Bruker AMX-400 MHz FT-NMR, and chemical shifts are reported in parts per million using tetramethylsilane (TMS) as an internal standard. The FT-IR spectra were measured as KBr disk on a Fourier transform infrared spectrometer, model Valor III from Jasco. The elemental analysis was carried out on a Heraeus CHN-Rapid elemental analyzer. The molecular weight and molecular weight distribution were determined by a gel permeation chromatography (GPC) using chloroform as eluent and monodisperse polystyrenes as standard. The thermogravimetric analysis (TGA) of the polymers was performed under nitrogen atmosphere at a heating rate of 20 °C/min using a Perkin–Elmer TGA-7 thermal analyzer. Thermal properties of the polymers were measured using a differential scanning calorimeter (DSC), Perkin–Elmer DSC-7, under nitrogen atmosphere at a heating rate of 10 °C/min.

Absorption spectra were measured with Jasco V-550 spectrophotometer and PL spectra were obtained using a Hitachi F-4500 fluorescence spectrophotometer. The voltammograms were recorded with a voltammetric analyzer (model CV-50W from BAS) at room temperature under nitrogen atmosphere. The measuring cell comprised glassy carbon as working electrode, Ag/AgCl electrode as reference electrode and platinum wire as auxiliary electrode, which were immersed in 0.1 M (*n*-Bu)₄NClO₄ in acetonitrile. The scan rate was 100 mV/s. The energy levels were calculated using the ferrocene (FOC) value of –4.8 eV with respect to vacuum level, which is defined as zero [31]. Atomic force microscope (AFM) images were obtained with a Veeco/Digital Instrument Scanning Probe Microscope (tapping mode) with Nanoscope IIIa controller.

The EL device configuration was ITO/PEDOT:PSS/P1–P6:Ir(ppy)₃:PBD/BCP (10 nm)/Ca (50 nm)/Al (100 nm), in which PBD (40 wt% of the copolymer) was incorporated to compensate for poor ability of the host material to transport electrons [13], and BCP [2,9-dimethyl-4,7-diphenyl-1,10-phenanthroline] was used as the hole-blocking layer [32]. The PLEDs were fabricated on pre-cleaned indium tin oxide (ITO) substrates with a sheet resistance of 14 Ω per square. The poly(3,4-ethylenedioxythiophene):poly(styrene sulfonate) (PEDOT:PSS) was first coated onto ITO glass as the hole-injection layer and annealed at 150 °C for 0.5 h in a dust-free atmosphere. The emitting layer comprising copolymer (20 mg), PBD (8 mg) and Ir(ppy)₃ (0.8 mg) was spin-coated onto the PEDOT:PSS layer from its solution in chlorobenzene (1 mL). And then, the hole-blocking layer (BCP) was deposited onto the polymeric film via thermal evaporation under ca. 2 × 10^{–6} Torr. Finally, the calcium and aluminum were deposited successively onto the BCP film as cathode via thermal evaporation under ca. 5 × 10^{–7} Torr. The film thicknesses of emissive layers were about 112–126 nm as measured by the AFM. For the measurements of device characteristics, the current density–voltage–luminance (*J*–*V*–*L*) changes and EL spectra were measured using a power supply (Keithley 2400) and a fluorescence spectrophotometer (Ocean Optics usb2000), respectively.

2.2. Polymer synthesis (Scheme 1)

Copolymers P1–P6 were synthesized by free radical polymerization of 4-vinyltriphenylamine (**1**) and 9-vinylcarbazole (**2**) using AIBN as an initiator. For example, to a solution of **1** (0.678 g, 2.5 mmol) and **2** (0.483 g, 2.5 mmol) in NMP (3 mL) was added with AIBN (24 mg). The solution was purged with dry nitrogen for 30 min, stirred at 85 °C for 24 h, and then poured into 200 mL of methanol. The appearing precipitates were collected by the centrifugal sedimentation and then purified by extracting with methanol for 24 h using a Soxhlet extractor. Thus-obtained polymer was further purified by being dissolved in CHCl₃ and reprecipitated from methanol several times. The product was collected by the centrifugal sedimentation and dried *in vacuo* to give a white



Scheme 1.

powder of **P1**. Yield was 60%. FT-IR (KBr pellet, cm^{-1}): ν 3083, 3062, 3028, 3003 (C–H stretch), 2922, 2852 (C–H stretch), 1589, 1509, 1490 (aromatic C=C). $^1\text{H NMR}$ (CDCl_3 , ppm): δ 7.27–6.56 (m, Ar H), 2.18–1.56 (m, $-\text{CH}_2-\text{CH}-$). Anal. Calcd. (%) for $(\text{C}_{19.28}\text{H}_{16.52}\text{N})_n$: C, 88.34; H, 6.31; N, 5.35. Found: C, 87.73; H, 6.34; N, 5.56.

Other copolymers (**P2–P6**) were prepared by a procedure analogous to **P1** using different feed ratios of **1** and **2**, and the obtained products were white powders with yields around 50–84%.

2.2.1. Polymer P2

Yield = 50%. FT-IR (KBr pellet, cm^{-1}): ν 3085, 3063, 3034, 3026, 3006 (C–H stretch), 2925, 2852 (C–H stretch), 1590, 1505, 1493 (aromatic C=C). $^1\text{H NMR}$ (CDCl_3 , ppm): δ 7.25–6.55 (m, Ar H), 2.17–1.56 (m, $-\text{CH}_2-\text{CH}-$). Anal. Calcd. (%) for $(\text{C}_{18.44}\text{H}_{15.96}\text{N})_n$: C, 88.08; H, 6.35; N, 5.57. Found: C, 87.40; H, 6.32; N, 5.62.

2.2.2. Polymer P3

Yield = 53%. FT-IR (KBr pellet, cm^{-1}): ν 3082, 3057, 3035, 3025 (C–H stretch), 2925, 2855 (C–H stretch), 1593, 1508, 1490 (aromatic C=C). $^1\text{H NMR}$ (CDCl_3 , ppm): δ 7.80–6.56 (m, Ar H), 1.95–1.28 (m, $-\text{CH}_2-\text{CH}-$). Anal. Calcd. (%) for $(\text{C}_{17.9}\text{H}_{15.6}\text{N})_n$: C, 87.89; H, 6.38; N, 5.73. Found: C, 86.76; H, 6.16; N, 5.98.

2.2.3. Polymer P4

Yield = 84%. FT-IR (KBr pellet, cm^{-1}): ν 3082, 3058, 3023 (C–H stretch), 2925, 2852 (C–H stretch), 1593, 1508, 1487 (aromatic C=C). $^1\text{H NMR}$ (CDCl_3 , ppm): δ 7.71–6.52 (m, Ar H), 2.04–1.22 (m, $-\text{CH}_2-\text{CH}-$). Anal. Calcd. (%) for $(\text{C}_{16.7}\text{H}_{14.8}\text{N})_n$: C, 87.43; H, 6.46; N, 6.11. Found: C, 86.84; H, 6.10; N, 6.58.

2.2.4. Polymer P5

Yield = 80%. FT-IR (KBr pellet, cm^{-1}): ν 3055, 3021, 2966 (C–H stretch), 2931, 2852 (C–H stretch), 1596, 1508, 1483 (aromatic C=C). $^1\text{H NMR}$ (CDCl_3 , ppm): δ 7.69–6.41 (m, Ar H), 2.09–1.25 (m, $-\text{CH}_2-\text{CH}-$). Anal. Calcd. (%) for $(\text{C}_{15.26}\text{H}_{13.84}\text{N})_n$: C, 86.80; H, 6.64; N, 6.56. Found: C, 86.12; H, 6.76; N, 5.98.

2.2.5. Polymer P6

Yield = 84%. FT-IR (KBr pellet, cm^{-1}): ν 3058, 3022, 2969 (C–H stretch), 2928, 2855 (C–H stretch), 1596, 1508, 1482 (aromatic C=C). $^1\text{H NMR}$ (CDCl_3 , ppm): δ 7.70–6.39 (m, Ar H), 2.04–1.24 (m, $-\text{CH}_2-\text{CH}-$). Anal. Calcd. (%) for $(\text{C}_{14.66}\text{H}_{13.44}\text{N})_n$: C, 86.50; H, 6.61; N, 6.89. Found: C, 86.33; H, 5.92; N, 7.10.

3. Results and discussion

3.1. Synthesis and characterization

The copolymers **P1–P6** were successfully prepared by copolymerization of 9-vinylcarbazole (**2**) and 4-vinyltriphenylamine (**1**) using AIBN as an initiator (Scheme 1). The polymerization results and characterization of the copolymers are summarized in Table 1. The actual compositions of 4-vinyltriphenylamine in copolymers are greater than those in monomer feeds, indicating that 4-vinyltriphenylamine is more reactive than 9-vinylcarbazole in radical copolymerization. The molar contents of 4-vinyltriphenylamine unit in **P1–P6** vary from 88 to 11%. The composition of the copolymers was estimated from their $^1\text{H NMR}$ spectra and confirmed by the EA data. For example, $^1\text{H NMR}$ spectra of copolymer **P5** and homopolymer **PTPA** are shown in Fig. 2. The chemical shifts at 4.94 and 7.69 ppm are attributed to the aromatic ring of the carbazole unit containing protons H-1, H-4 and H-5 [38], from whose areas the ratios of the incorporated comonomers in host copolymer were determined. The copolymers were readily soluble in common organic solvents such as toluene, chloroform, THF, and 1,1,2,2-tetrachloroethane; their weight-average molecular weights

Table 1
Polymerization results and characterization of **P1–P6**

No.	Feed ratio ^a	Composition in copolymer ^b (x:y)	Yield (%)	M_n^c ($\times 10^4$)	M_w^c ($\times 10^4$)	PDI ^c	T_d^d ($^\circ\text{C}$)	T_g ($^\circ\text{C}$)
P1	5:5	0.12:0.88	60	1.34	2.24	1.67	410	145.4
P2	6:4	0.26:0.74	50	1.18	1.81	1.53	407	146.4
P3	7:4	0.35:0.65	53	1.33	2.06	1.55	404	159.1
P4	7:3	0.55:0.45	84	0.89	1.50	1.69	402	185.4
P5	8:2	0.79:0.21	80	0.92	1.41	1.53	425	– ^e
P6	9:1	0.89:0.11	84	0.91	1.72	1.89	432	– ^e

^a Feed molar ratio = 9-vinylcarbazole:4-vinyltriphenylamine.

^b The compositions were estimated from $^1\text{H NMR}$ spectra. x:y = the ratio of pendant carbazole to triphenylamine.

^c M_n , M_w , and PDI were determined by gel permeation chromatography using polystyrene standard in CHCl_3 .

^d The temperature at 5% weight loss.

^e No obvious T_g was observed in DSC thermogram.

(M_w s), determined by GPC using monodisperse polystyrene as standard, were 2.24×10^4 , 1.81×10^4 , 2.06×10^4 , 1.50×10^4 , 1.41×10^4 , and 1.72×10^4 , respectively. These copolymers exhibited good thermal stability with thermal decomposition temperature (T_d) above 400°C under nitrogen atmosphere. On DSC thermograms, **P1–P4** revealed the glass transition temperatures (T_g s) at 145.4, 146.4, 159.1, and 185.4°C , respectively. However, for **P5** and **P6**, no obvious glass transition temperature (T_g) was observed below 250°C . The high T_g values of the present host copolymers (145.4 – 185.4°C) are expected to prevent morphology deformation and degradation when used as emitting layer in PLEDs. Variations in morphology due to low glass transition temperatures upon device operation are believed to be the main causes of degradation [33].

3.2. Optical properties

Fig. 1 shows the chemical structures of the host materials (**P1–P6**, **PVK** and **PTPA**), green phosphor [$\text{Ir}(\text{ppy})_3$], BCP, PBD and device structure of the PLEDs fabricated for optoelectronic investigation. Fig. 3(a) shows the absorption spectra of **P1–P6**, **PVK** and **PTPA**

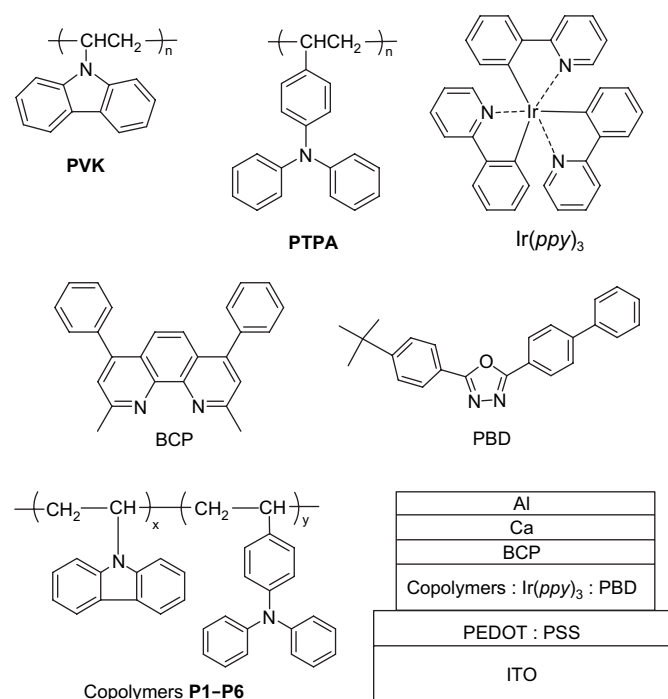


Fig. 1. Chemical structures of the materials used in this work and structure of the single-emitting-layer PLED.

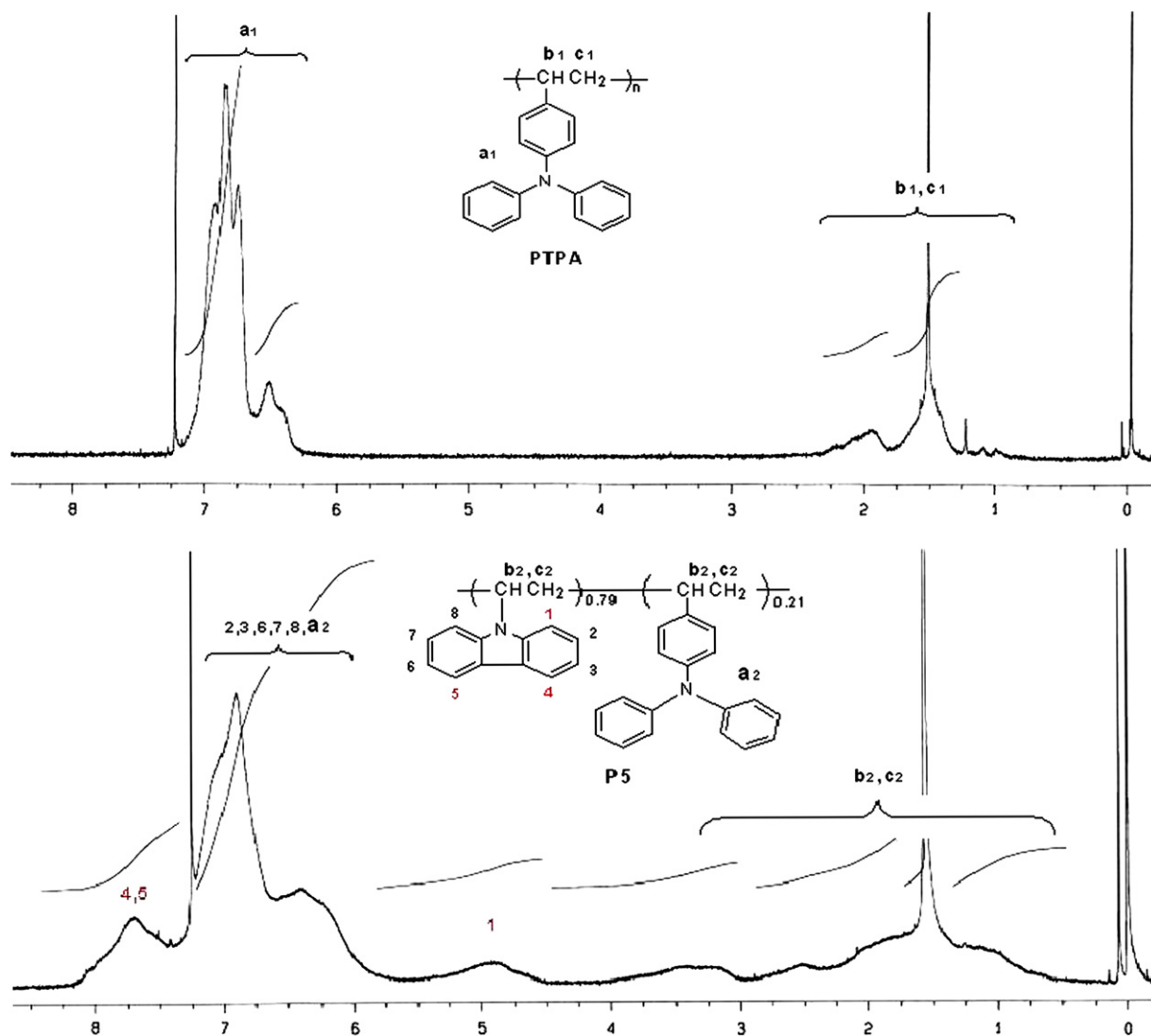


Fig. 2. ^1H NMR spectra of PTPA and P5.

coated on quartz plate. The maximum absorption of **PVK** and **PTPA** is 295 and 312 nm, respectively, which is originated from the π - π^* electronic transitions of the side chromophores (carbazole or triphenylamine). Moreover, there are shoulders (ca. 320–350 nm) in the absorption spectrum of the **PVK**. The maximum absorption of the **P1–P6** is 309, 307, 304, 298, 296 and 295 nm, respectively, which can also be attributed to the π - π^* electronic transitions of the pendant chromophores. The absorption bands blue-shift gradually with an increase in carbazole content (12 mol% \rightarrow 89 mol%). The spectra of **P5** and **P6** show extra shoulders at ca. 340 nm. Clearly, the spectral features of the copolymers (**P5**, **P6**) become similar to that of **PVK** at high carbazole content. As shown in Fig. 3(b), the absorption spectrum of $\text{Ir}(\text{ppy})_3$ film shows strong absorption at 290 nm originated from the ligand-centered π - π^* transition, with weaker absorptions at 340–380 and 460 nm attributed to the singlet metal-to-ligand charge transfer ($^1\text{MLCT}$) and triplet metal-to-ligand charge transfer ($^3\text{MLCT}$) transitions, respectively. [34] The PL spectrum of $\text{Ir}(\text{ppy})_3$ film shows an emission peak at 517 nm, which is attributed to $^3\text{MLCT}$ transition. The probability of Förster energy transfer from the host to phosphor is enhanced by the degree of spectral overlap between donor's PL band and acceptor's absorption band. As shown in Fig. 3(b), PL band of **P1–P6** overlaps with absorption band of $\text{Ir}(\text{ppy})_3$ at ca. 350–500 nm (MLCT transitions), suggesting that efficient energy transfer from **P1–P6** to

$\text{Ir}(\text{ppy})_3$ would occur. In order to study the efficiency of Förster energy transfer between **P1–P6** and $\text{Ir}(\text{ppy})_3$, the PL spectra of the blend films prepared from **P1** to **P6** doped with 4 wt% $\text{Ir}(\text{ppy})_3$ under photo-excitation were investigated (Fig. 4). The emissions of **P1–P6** (peaks at 375 and 440 nm) degenerate significantly and mainly that of $\text{Ir}(\text{ppy})_3$ at 517 nm is observed. Moreover, the relative PL spectral intensity of **P1–P6** below 470 nm is smaller than that of **PTPA**, suggesting that the energy transfer to $\text{Ir}(\text{ppy})_3$ is more efficient for the copolymers containing triphenylamine groups.

In a phosphorescent device, triplet energy (E_T) of host should be larger than that of phosphor to improve the efficiency of triplet-triplet energy transfer [35]. Therefore, it is required to determine the E_T of our hosts and compare with that of conventional **PVK**. Phosphorescent spectra of **P1–P6** and **PVK** were obtained at 77 K in a frozen solution of CHCl_3 as shown in Fig. 5. The peak of the shortest wavelength of the phosphorescence spectra is assigned as triplet energy state (E_T). As summarized in Table 2, the E_T s of **P1–P6** are 2.73, 2.89, 2.89, 2.90, 2.89 and 2.89 eV, respectively, while that of **PVK** is 2.49 eV [36]. When determined using film samples at 77 K, the E_T s of **P1–P6** are 2.59, 2.72, 2.73, 2.74, 2.74 and 2.74 eV, respectively. The E_T s of **P1–P6** are higher than that of $\text{Ir}(\text{ppy})_3$ (2.6 eV) [37], ensuring that the triplet energy transfer from **P1–P6** to $\text{Ir}(\text{ppy})_3$ is exothermic system and should be effective in suppressing back energy transfer from $\text{Ir}(\text{ppy})_3$ to hosts **P1–P6**.

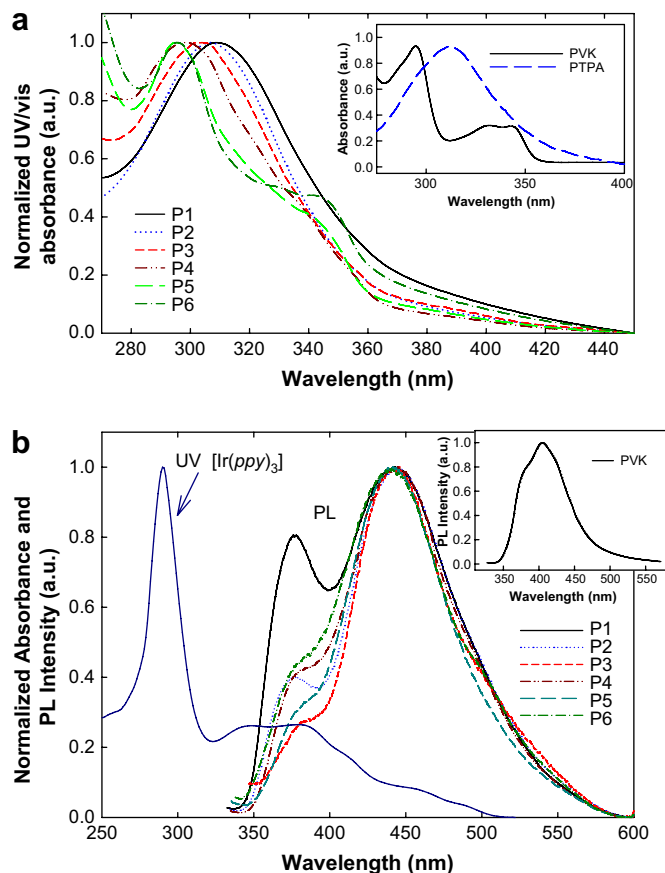


Fig. 3. (a) Absorption and (b) photoluminescence spectra of **P1–P6** films coated on quartz plate. The insets in (a) and (b) are the absorption of **PVK**, **PTPA** and PL spectra of **PVK**, respectively.

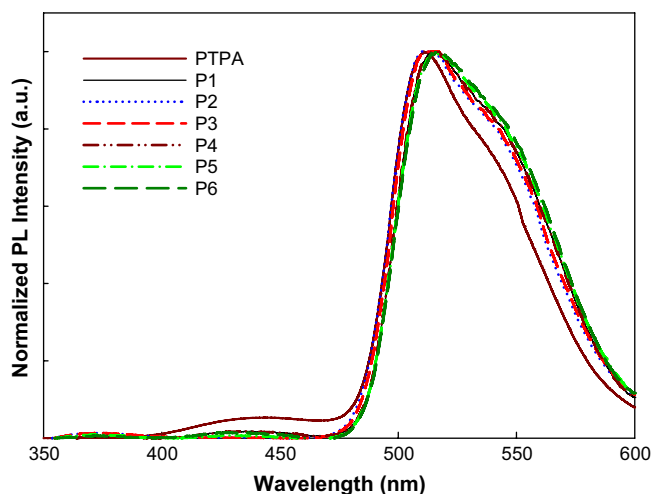


Fig. 4. PL spectra of the blend films prepared from **P1** to **P6** doped with 4 wt% $\text{Ir}(\text{ppy})_3$ ($\lambda_{\text{ex}} = 310 \text{ nm}$).

3.3. Electrochemical properties

The HOMO energy levels of **P1–P6** films were estimated from their cyclic voltammograms using the equation $E_{\text{HOMO}} = -(E_{\text{onset}} + 4.8) \text{ eV}$, where E_{onset} is the onset oxidation potential relative to the ferrocene/ferrocenium couple. **Fig. 6** shows the cyclic voltammograms (CVs) of **P1–P6** films coated on a glassy carbon electrode in anodic scan, with the corresponding electrochemical data summarized in **Table 3**. The

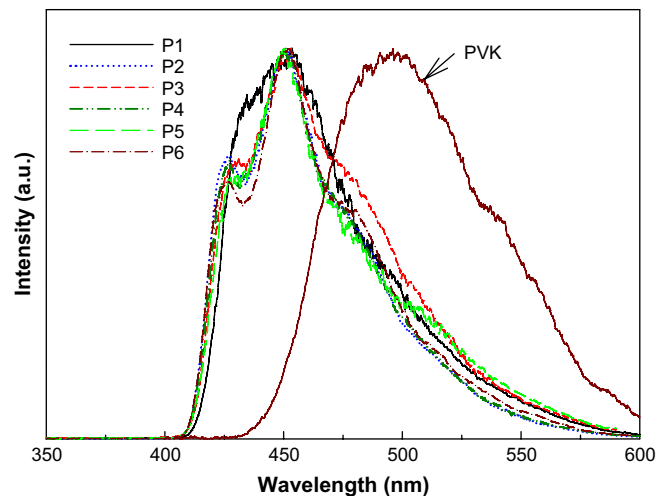


Fig. 5. Phosphorescent spectra of **P1–P6** and **PVK** solutions in CHCl_3 (measured at 77 K).

Table 2
Triplet energy state of **P1–P6** and **PVK**

No.	First peak in spectra (nm)	E_{T} (eV)
P1	454	2.73
P2	429	2.89
P3	429	2.89
P4	427	2.90
P5	429	2.89
P6	429	2.89
PVK	497	2.49

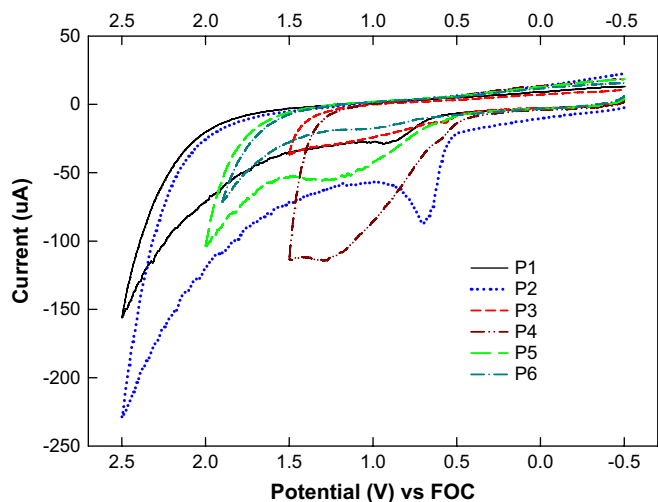


Fig. 6. Cyclic voltammograms of **P1–P6** films coated on carbon electrode (scan rate: 100 mV/s).

Table 3
Electrochemical data of **P1–P6**

No.	$E_{\text{onset}}(\text{ox})$ (V) versus FOC	$E_{\text{HOMO}}^{\text{a}}$ (eV)	$E_{\text{LUMO}}^{\text{b}}$ (eV)	$E_{\text{g}}^{\text{opt c}}$ (eV)
P1	0.62	−5.42	−2.02	3.37
P2	0.52	−5.32	−1.92	3.40
P3	0.40	−5.20	−1.80	3.40
P4	0.38	−5.18	−1.79	3.39
P5	0.48	−5.28	−1.89	3.39
P6	0.53	−5.33	−1.96	3.37

^a $E_{\text{HOMO}} = -e(E_{\text{onset}}(\text{ox})_{\text{FOC}} + 4.8 \text{ V})$.

^b $E_{\text{LUMO}} = E_{\text{HOMO}} + E_{\text{g}}^{\text{opt}}$.

^c Optical band gaps obtained from UV–vis absorption spectra.

onset oxidation potentials of **P1–P6** are at 0.62, 0.52, 0.40, 0.38, 0.48, and 0.53 V, respectively. The HOMO energy levels of **P1–P6** calculated from their onset oxidation potentials are -5.42 , -5.32 , -5.20 , -5.18 , -5.28 , and -5.33 eV, respectively, which are higher than that of **PVK** (-5.8 eV). This seems to be attributed to stronger hole-affinity of pendant triphenylamine groups. The HOMO energy level of **PTPA** is estimated to be -5.36 eV from the onset oxidation potential. Accordingly, the energy barrier for hole injection between the PEDOT:PSS and emitting layer can be effectively reduced. Moreover, the HOMO levels of the copolymers (**P1–P6**) vary with their compositions. Among them, **P4** reveals the highest HOMO energy level (-5.18 eV), suggesting that a higher HOMO energy level is readily obtained when the molar contents of pendant carbazole and triphenylamine groups are coming close to one another. The LUMO energy levels of **P1–P6**, calculated from the HOMO energy levels and the optical energy gaps are -2.02 , -1.92 , -1.80 , -1.79 , -1.89 , and -1.96 eV, respectively. The energy band diagrams of **P4**, **PVK**, **Ir(ppy)₃**, and **BCP** are shown in Fig. 7. The HOMO energy level of the host **PVK** (-5.8 eV) [36] is lower than that of **Ir(ppy)₃** (-5.6 eV), resulting in holes trapping in **Ir(ppy)₃**. In contrast, higher HOMO energy levels of **P1–P6** (-5.18 to -5.42 eV) prevent the holes trapping in phosphor to improve the holes injection and transport. Among them, **P4** shows the highest HOMO level (-5.18 eV), which should result in better device performance than other copolymers.

3.4. Electroluminescent properties

Fig. 8 shows the EL spectra of the EL devices (ITO/PEDOT:PSS/**P1–P6**:**Ir(ppy)₃**:PBD/BCP/Ca/Al) containing blend films of **P1–P6** and PBD (40 wt% of host copolymer) doped with **Ir(ppy)₃** (4 wt%) as emitting layer. The emission peak at 517 nm is attributed exclusively to **Ir(ppy)₃**, indicating that the emissions of **P1–P6** are completely quenched (see Fig. 4). The shoulder peaks at short wavelength (400–475 nm) in PL spectra disappear completely. This is probably owing to simultaneous occurrence of carriers trapping at **Ir(ppy)₃** in addition to normal energy transfer (Förster and Dexter) from the host to **Ir(ppy)₃**. The results suggest that **P1–P6** are excellent host materials for these device systems, in which the exciton energy can be completely transferred to the green phosphor **Ir(ppy)₃**. Moreover, as shown in Fig. 8, the full width at half maximum (FWHM) of **P4** in EL spectra is the narrowest (80 nm), as compared with ca. 90 nm of other copolymers (**P1–P3**, **P5**, **P6**). Therefore, purer green light can be obtained using **P4** as the host material. Fig. 9 shows the current density versus bias characteristics for the EL devices, with inset showing the luminance versus current density characteristics. Under the same bias, an increase in molar contents of triphenylamine groups (11 mol% → 88 mol% in

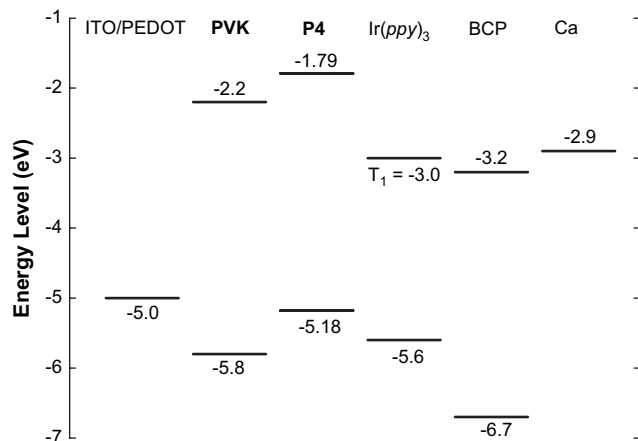


Fig. 7. The energy band diagram of **P4**, **Ir(ppy)₃**, **BCP**, and **PVK**.

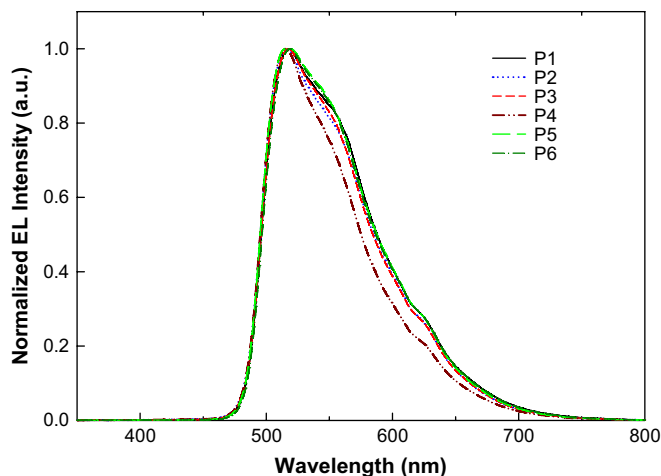


Fig. 8. EL spectra of the blend films prepared from **P1** to **P6** doped with **Ir(ppy)₃** (4 wt%).

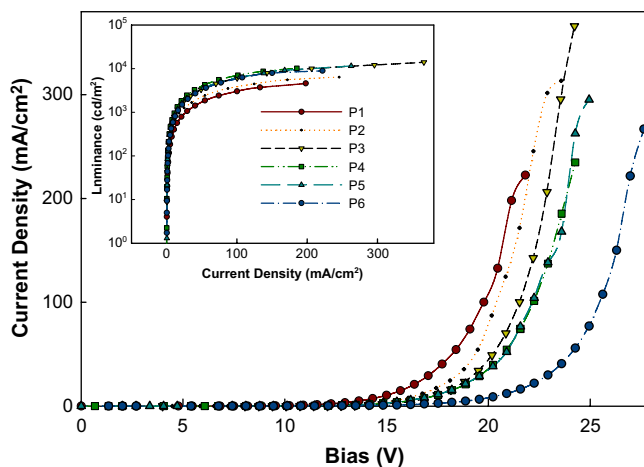


Fig. 9. The current density versus bias characteristics for the EL devices (ITO/PEDOT:PSS/**P1–P6**:**Ir(ppy)₃**:PBD/BCP/Ca/Al) prepared from **P1** to **P6** doped with 4 wt% **Ir(ppy)₃**. The inset shows the luminance versus current density characteristics.

P6 → **P1**) leads to increased current density of the EL devices, confirming that the triphenylamine groups are effective in enhancing hole transporting ability. The EL performance data of all devices prepared from **P1** to **P6** or **PVK** doped with **Ir(ppy)₃** are summarized in Table 4. The best performance was obtained for the device based on **P4**, in which the maximum luminance (L_{\max}) and the maximum luminance efficiency (LE_{\max}) are 11501 cd/m^2 and 10.6 cd/A , respectively. The L_{\max} and LE_{\max} of **P1–P6** are 4575, 6372, 10286, 11501, 9581, 8906 cd/m^2 and 3.8, 5.7, 9.4, 10.6, 8.6, 6.8 cd/A , respectively. The L_{\max} and LE_{\max} of **PTPA** device are 9219 cd/cm^2

Table 4
Performance of the EL devices prepared from **P1** to **P6** or **PVK** doped with **Ir(ppy)₃**^a

Host polymer	Thickness (nm)	L_{\max}^b (cd/m^2)	Bias ^c (V)	LE_{\max}^b (cd/A)	CIE coordinates ^d (x, y)
P1	126	4574	21.1	3.8	(0.38, 0.57)
P2	121	6372	20.8	5.7	(0.37, 0.57)
P3	124	10286	19.5	9.4	(0.38, 0.56)
P4	126	11501	23.6	10.6	(0.36, 0.58)
P5	120	9581	24.2	8.6	(0.37, 0.57)
P6	113	8906	26.9	6.8	(0.38, 0.57)
PVK	112	2560	22.9	2.4	(0.36, 0.58)

^a EL configuration: ITO/PEDOT:PSS/**P1–P6** or **PVK**:**Ir(ppy)₃**:PBD/BCP/Ca/Al.

^b L_{\max} : maximum luminance; LE_{\max} : maximum luminance efficiency.

^c Bias at maximum luminance.

^d At a bias of 18.4 V.

and 6.1 cd/A. The L_{\max} and LE_{\max} of **P4** device are almost four times to those of **PVK** device, suggesting that the composition of **P4** should play an important role in enhancing the EL performance. Unfortunately, the real mechanism of this composition-dependent optoelectronic performance in **P1–P6** devices has not been elucidated so far. However, the enhancement in L_{\max} and LE_{\max} for **P4** (4-vinyltriphenylamine:9-vinylcarbazole = 45:55) is probably attributable to reduced excimer/exciplex formation. The higher efficiency of the devices based on **P1–P6** (3.8–10.6 cd/A) than that of **PVK** (2.4 cd/A) can also be attributed to easier hole injection and enhanced hole transport, which is mainly contributed by hole-affinitive triphenylamine groups.

4. Conclusion

We have successfully synthesized copolymers **P1–P6** containing pendant hole-transporting triphenylamine and carbazole groups by radical copolymerization. The copolymers possess moderate molecular weight ($M_w = 14\,100$ – $22\,400$, PDI = 1.53–1.89) and are soluble in common organic solvents such as toluene, chloroform, THF, and 1,1,2,2-tetrachloroethane. Their decomposition temperatures (T_{ds}) and glass transition temperatures (T_{gs}) are 402–432 °C and 145.4–185.4 °C, respectively. The PL spectra of their blend with green phosphor Ir(ppy)₃ under photo-excitation ($\lambda_{ex} = 310$ nm) show evidence of efficient energy transfer from **P1–P6** to Ir(ppy)₃. The higher triplet energy of **P4** ($E_T = 2.90$ eV) than that of Ir(ppy)₃ ($E_T = 2.6$ eV) ensures that the triplet energy transfer from **P4** to Ir(ppy)₃ is exothermic system. The copolymers **P1–P6** show higher HOMO levels (–5.18 to –5.42 eV) relative to **PVK** (–5.8 eV) due to high hole-affinity of the pendant triphenylamine groups. The phosphorescent EL devices [ITO/PEDOT:PSS/**P1–P6**:Ir(ppy)₃:PBD/BCP/Ca/Al] emit 517 nm light attributed exclusively to Ir(ppy)₃. Their maximum luminance and luminance efficiency are 4574–11501 cd/m² and 3.8–10.6 cd/A, respectively, which are significantly enhanced when compared with those of **PVK** device (2560 cd/m², 2.4 cd/A). Among them, **P4** device shows the best performance (11501 cd/m², 10.6 cd/A). Current results reveal that copolymers **P1–P6** are promising host materials for phosphorescent light-emitting diodes.

Acknowledgments

The authors thank the National Science Council of Taiwan for the financial aid through project NSC 95-2221-E-006-226-MY3.

References

- [1] Burroughes JH, Bradley DDC, Brown AR, Marks RN, Macay K, Friend RH, et al. *Nature* 1990;347:539.
- [2] Baldo MA, O'Brien DF, You Y, Shoustikov A, Sibley S, Thompson ME, et al. *Nature* 1998;395:151.
- [3] Baldo MA, Thompson ME, Forrest SR. *Nature* 2000;403:750.
- [4] Tokito S, Iijima T, Suzuri Y, Kita H, Tsuzuli T, Sato F. *Appl Phys Lett* 2003; 83:569.
- [5] Baldo MA, Lamansky S, Burrows PE, Thompson ME, Forrest SR. *Appl Phys Lett* 1999;75:4.
- [6] Kawamura Y, Goushi K, Brooks J, Brown JJ, Sasabe H, Adachi C. *Appl Phys Lett* 2005;86:071104.
- [7] Lee CL, Lee KB, Kim JJ. *Appl Phys Lett* 2000;77:2280.
- [8] Yang MJ, Tsutsui T. *Jpn J Appl Phys* 2000;39:828.
- [9] Vaeth KM, Tang CW. *J Appl Phys* 2002;92:3447.
- [10] Yang X, Neher D, Hertel D, Däubler TK. *Adv Mater* 2004;16:161.
- [11] Gong X, Ostrowski JC, Bazan GC, Moses D, Heeger AJ, Liu MS, et al. *Adv Mater* 2003;15:45.
- [12] Gong X, Lim SH, Ostrowski JC, Moses D, Bardeen CJ, Bazan GC. *J Appl Phys* 2004;95:948.
- [13] Jiang C, Yang W, Peng J, Xiao S, Cao Y. *Adv Mater* 2004;16:537.
- [14] Kavitha J, Chang SY, Chi Y, Yu JK, Hu YH, Chou PT, et al. *Adv Funct Mater* 2005;15:223.
- [15] Tung YL, Lee SW, Chi Y, Chen LS, Shu CF, Wu FI, et al. *Adv Mater* 2005;17:1059.
- [16] Klessinger M, Michl J. *Excited states and photochemistry of organic molecules*. New York: Wiley-VCH; 1995.
- [17] Adachi C, Kwong RC, Djurovich P, Adamovich V, Baldo MA, Thompson ME, et al. *Appl Phys Lett* 2001;79:2082.
- [18] Yang XH, Jaiser F, Klinger S, Neher D. *Appl Phys Lett* 2006;88:21107.
- [19] Chen XW, Liao JL, Liang YM, Ahmed MO, Tseng HE, Chen SA. *J Am Chem Soc* 2003;125:636.
- [20] Jiang J, Jiang C, Yang W, Zhen H, Huang F, Cao Y. *Macromolecules* 2005; 38:4072.
- [21] You Y, Kim SH, Jung HK, Park SY. *Macromolecules* 2006;39:349.
- [22] Schulz GL, Chen X, Chen SA, Holdcroft S. *Macromolecules* 2006;39:9157.
- [23] Sandee AJ, Williams CK, Evans NR, Davies JE, Boothby CE, Köhler A, et al. *J Am Chem Soc* 2004;126:7041.
- [24] Zhen H, Jiang C, Yang W, Jiang J, Huang F, Cao Y. *Chem Eur J* 2005;11:5007.
- [25] Noh YY, Lee CL, Kim JJ, Yase K. *J Chem Phys* 2003;118:2853.
- [26] Shirota Y, Kuwabara Y, Inada H, Wakimoto T, Nakada H, Yonemoto Y, et al. *Appl Phys Lett* 1994;65:807.
- [27] Shirota Y, Kobata T, Noma N. *Chem Lett* 1989:1145.
- [28] Ikai M, Tokito S, Sakamoto Y, Suzuki T, Taga Y. *Appl Phys Lett* 2001;79:156.
- [29] Kuwabara Y, Ogawa H, Shirota Y. *Adv Mater* 1994;6:677.
- [30] Yeh KM, Lee CC, Chen Y. *Synth Met*, in press.
- [31] Liu Y, Liu MS, Jen AKY. *Acta Polym* 1999;50:105.
- [32] D'Andrade BW, Thompson ME, Forrest SR. *Adv Mater* 2002;14:147.
- [33] Qiu Y, Qiao J. *Thin Solid Films* 2000;372:265.
- [34] Lamansky S, Djurovich P, Murphy D, Abdel-Razzaq F, Lee HE, Adachi C, et al. *J Am Chem Soc* 2001;123:4304.
- [35] Liu QD, Lu J, Ding J, Day M, Tao Y, Barrios P, et al. *Adv Funct Mater* 2007; 17:1028.
- [36] Kawamura Y, Yanagida S, Forrest SR. *J Appl Phys* 2002;92:87.
- [37] Adachi C, Baldo MA, Thompson ME, Forrest SR. *J Appl Phys* 2001;90:5048.
- [38] Karali A, Froudakis GE, Dais P. *Macromolecules* 2000;33:3180.